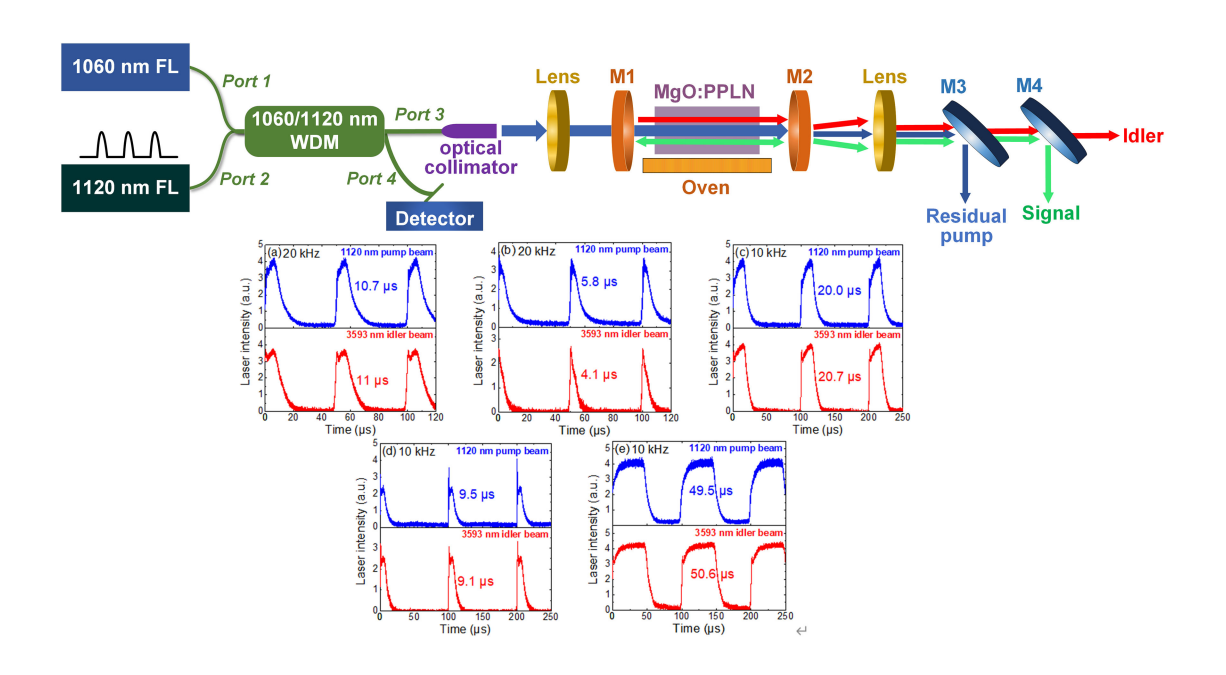


**3**Open Access

# Highly-Efficient Pulsed Mid-Infrared Generation Based on Intracavity Difference Frequency Mixing

Volume 13, Number 3, June 2021

Peng Wang Xiao Li Kaifeng Wang Xiaojun Xu



DOI: 10.1109/JPHOT.2021.3073622





# Highly-Efficient Pulsed Mid-Infrared Generation Based on Intracavity Difference Frequency Mixing

Peng Wang <sup>(1)</sup>, <sup>1,2,3</sup> Xiao Li <sup>(1)</sup>, <sup>1,2,3</sup> Kaifeng Wang, <sup>1,2,3</sup> and Xiaojun Xu<sup>1,2,3</sup>

<sup>1</sup>College of Advanced Interdisciplinary Studies, National University of Defense Technology, Changsha 410073, China

DOI:10.1109/JPHOT.2021.3073622

This work is licensed under a Creative Commons Attribution 4.0 License. For more information, see https://creativecommons.org/licenses/by/4.0/

Manuscript received February 10, 2021; revised April 1, 2021; accepted April 13, 2021. Date of publication April 15, 2021; date of current version April 28, 2021. This work was supported in part by Open Research Fund of State Key Laboratory of Pulsed Power Laser Technology, Electronic Countermeasure Institute, National University of Defense Technology under Grant SKL2020ZR03 and in part by the National Natural Science Foundation of China under Grant 61975236. Corresponding author: Xiao Li (e-mail: Crazy,li@163.com).

**Abstract:** We demonstrated highly-efficient pulsed mid-infrared generation based on intracavity difference frequency mixing inside a continuous-wave (CW) PPLN optical parametric oscillator (OPO). The near-infrared pulsed fiber source was located at 1120 nm with variable pulse width and repetition rate. The pump source of OPO was a CW linearly-polarized highpower 1060 nm fiber laser. The 1120 nm and 1060 nm pump beams were simultaneously incident into the OPO cavity. The 1060 nm pump beam built parametric oscillation firstly and generated high-power resonant signal beam inside the cavity. By controlling the PPLN temperature properly, the phase-matched difference frequency generation (DFG) occurred between the signal beam and 1120 nm pulsed pump beam in the PPLN crystal. Finally, the pulsed 1120 nm pump beam was successfully transformed to 3593 nm mid-infrared radiation at every power level and temporal characteristic. Both the slope efficiency and pump-to-idler conversion efficiency of the intracavity DFG process reached over 20%. In addition, the pulse shape of newly generated 3593 nm idler beam was basically the same as 1120 nm pump beam. The experimental results exhibited huge potential in frequency down conversion of low-power laser sources with special temporal characteristics.

Index Terms: Infrared lasers, fiber lasers, nonlinear crystals, nonlinear.

## 1. Introduction

The pulsed laser sources operating in the 3  $\sim$  5  $\mu$ m mid-infrared range have many particular characteristics such as containing important transparent window of the atmosphere and nearly all fundamental rovibrational absorption bands of molecules, and have been widely used in many application fields such as defense, laser microsurgery, mid-infrared spectroscopy, remote communication [1]–[4]. Benefitting from simple structure, strong expandability and excellent tuning performance, the nonlinear frequency down-conversion including OPO and DFG using the PPLN crystals has become one of the most promising candidates to generate pulsed mid-infrared

<sup>&</sup>lt;sup>2</sup>State Key Laboratory of Pulsed Power Laser Technology, National University of Defense Technology, Changsha 410073, China

<sup>&</sup>lt;sup>3</sup>Hunan Provincial Key Laboratory of High Energy Laser Technology, Changsha 410073, China

radiation. In 2015, Yuefeng Peng et al reported on a high-power, narrow-linewidth OPO which was pumped by a 310 W pulsed Nd:YAG master oscillator power amplifier (MOPA) laser located at 1064 nm and obtained 71.6 W pulsed mid-infrared radiation at 2.907  $\mu$ m with a slope efficiency of 26.7%, which was the highest output power for mid-infrared PPLN OPO [5]. In 2018, S. Parsa et al demonstrated the first picosecond idler-resonant PPLN OPO which was pumped by a 1064 nm mode-locked fiber laser with the average power of 11 W and realized widely tunable mid-infrared radiation across 2198-4070 nm [6]. However, the OPO usually requires that the output power of pump source reaches the oscillation threshold. For the case of low-power pulsed fiber seed, the MOPA structure is generally used for power amplification. But in the amplifier stage, the negative fiber nonlinear effects are easy to be induced and threaten the safety of the whole pump source, especially the fiber seed. On the contrary, the DFG scheme is typically a single-pass process which is non-resonant and doesn't need a resonant cavity, significantly low reflectance on the crystal surfaces, complicated coatings on mirrors or critical cavity alignment to initiate. It usually adopts a high-power laser source around 1.5  $\mu$ m to interact with the 1  $\mu$ m pulsed laser for achieving frequency down-conversion. In 2015, Paul Belden et al demonstrated a pulsed mid-infrared laser source located at  $\sim$ 3520 nm with >1 W average power and up to 5  $\mu$ J pulse energy via DFG of a few-ns pulse, variable pulse-repetition 1064 nm fiber laser source and a 10 mW, continuous-wave 1525 nm single-frequency laser diode in a PPLN crystal [7]. In 2016, R. T. Murray et al reported on a high average power, picosecond-pulsed, mid-infrared DFG source concluding two synchronous MOPA systems. They obtained over 3.4 W idler power which can be tuned from 3.28  $\sim$  3.45  $\mu$ m and the maximum pump-to-idler conversion efficiency reached 26% [8]. However, the DFG scheme usually acquires a high-power 1.5  $\mu$ m laser source which was much harder to obtain, especially compared with the 1  $\mu$ m laser source. In addition, limited by single-pass interaction, the DFG scheme is normally less efficient than OPOs which makes it less suitable for applications that requires high conversion efficiency.

To overcome the drawbacks of DFG and OPO, combining them together in one resonant cavity and ensuring both of them satisfy phase-matching conditions is a novel method to achieve high conversion efficiency and excellent capacity of keeping time-domain characteristics, which was firstly put forward by our research group. Using this method, we have demonstrated highly efficient frequency down-conversion of 1018 nm and 1080 nm fiber lasers [9]. In this letter, we further investigated the applicability of this method in frequency down-conversion of long-wavelength, pulsed fiber source and obtained pulsed mid-infrared output. The pulsed fiber laser was located at 1120 nm and had a maximum average power of 5.64 W. Its repetition rate and pulse width could be tuned independently. A high-power 1060 nm continuous-wave (CW) fiber laser was adopted as the assisting laser. Two pump beams were simultaneously incident into the resonant cavity and a high-intensity signal beam was obtained inside the cavity. By controlling the crystal temperature properly, the 1120 nm pump beam was successfully transformed to 3593 nm mid-infrared radiation at every power level via the phase-matched DFG between it and the signal beam. Both the pumpto-idler conversion efficiency and slope efficiency reached over 20%. In addition, the temporal characteristics of 1120 nm pump beam was almost perfectly inherited by the 3593 nm idler beam except for one pumping situation. The experiment results verified the feasibility of highly-efficient frequency down-conversion relying on phase-matched DFG inside the OPO once again.

# 2. Experiment Setup

Fig. 1 described the schematic diagram of the experiment setup. The pump sources were two linearly-polarized home-made fiber lasers (FLs), one CW 1060 nm FL and one pulsed 1120 nm FL. The maximum output power of the 1060 nm FL was 67 W. Both the repetition rate and pulse width of the 1120 nm FL was tunable and its maximum average power reached 5.64 W. A polarization-maintaining 1060/1120 nm wavelength division multiplexer (WDM) was adopted to combine two FLs together. Two ports of the WDM, port 1 and port 2, were fused with 1060 nm and 1120 nm FLs separately and the pump beam was output from port 3. About tens of milliwatts pump radiation was output from port 4 for spectral measurement to monitor the working status of pump sources. A

Fig. 1. Schematic diagram of highly-efficient pulsed DFG inside the CW OPO.

fiber optical collimator was fused with the port 3 and delivered the collimated dual-wavelength (DW) pump beam with a beam radius of about 1 mm. The pump beam transmitted through a focusing lens with the focal length of 150 mm and was incident into the resonant cavity. The cavity was designed as a typical standing-wave structure, consisting of two curved mirrors, M1 and M2. Both two mirrors had a curvature radius of about 150 mm and the total cavity length was also set as 150 mm. Both two mirrors had anti-reflection (AR) coating (R < 5%) for the pump over 1  $\sim$  1.2  $\mu$ m and the idler over  $3 \sim 4 \ \mu m$ . For ensuring singly resonant oscillation for the signal beam, M1 was with the high-reflection (HR) coating (R>99%) for the signal over 1.4  $\sim$  1.7  $\mu$ m while M2 was the output coupling mirror with the 5% transmittance coating for the signal. In this experiment, we used a bulk of MgO-doped PPLN as the nonlinear crystal for frequency conversion. Its dimension was  $50 \times 10 \times 1$  mm<sup>3</sup> and had a period of 31.1  $\mu$ m. The PPLN crystal was placed in the middle of two cavity mirrors and the DW pump beam was focused in the center of it. Both two end-faces of PPLN was carefully polished and coated with high anti-reflection film for all three wavelength bands. An oven was placed under the cavity for controlling temperature of the PPLN crystal. After the cavity was another collimating lens used to adjust the output beam to be parallel for accurate measurement. Two dichroic mirrors, M3 and M4, were located behind the lens for separating the residual pump, signal and idler waves. The OPO system has been integrated and moduled with the fiber optical collimator as shown in Ref. [10] which guaranteed the reliability of experimental results under different conditions.

# 3. Experimental Results and Discussion

## 3.1. Determination of Appropriate Grating Period

In the experiment, the 1060 nm pump beam built parametric oscillation and the DFG occurred between the signal beam and 1120 nm pump beam. To increase its conversion efficiency, the grating period of PPLN crystal should be properly adjusted to ensure that the OPO and the DFG simultaneously satisfy phase-matching conditions. The tuning curves corresponding to 1060 nm and 1120 nm lasers at different crystal temperature were simulated based on the often-cited LiNbO3 Sellmeier equations from Edwards and Lawrence [11], and shown in Fig. 2. In the simulation, the grating period was set as 31.1  $\mu$ m and the crystal temperature ranged from 40 °C to 80 °C with the step of 2 °C. Fig. 2(a) reveals that in the signal range, two tuning curves just had one intersection point. The coordinate value of the data point closest to the intersection point was (60 °C, 1625 nm). Fig. 2(b) indicated that when the crystal temperature was set at 60 °C, the idler wavelength corresponding to 1060 nm and 1120 nm pump beams was 3048 nm and 3605 nm separately. The simulation result reveals that in order to achieve highly-efficient frequency down-conversion of pulsed 1120 nm radiation, the PPLN temperature should be controlled at 60 °C for ensuring phase-matched intracavity DFG.

## 3.2. Carrying Out Experiments Based on Simulation Results

According to the simulation results, the PPLN crystal should be heated to 60 °C and the signal wavelength would be 1625 nm. However, in the experiment, the signal wavelength was a little

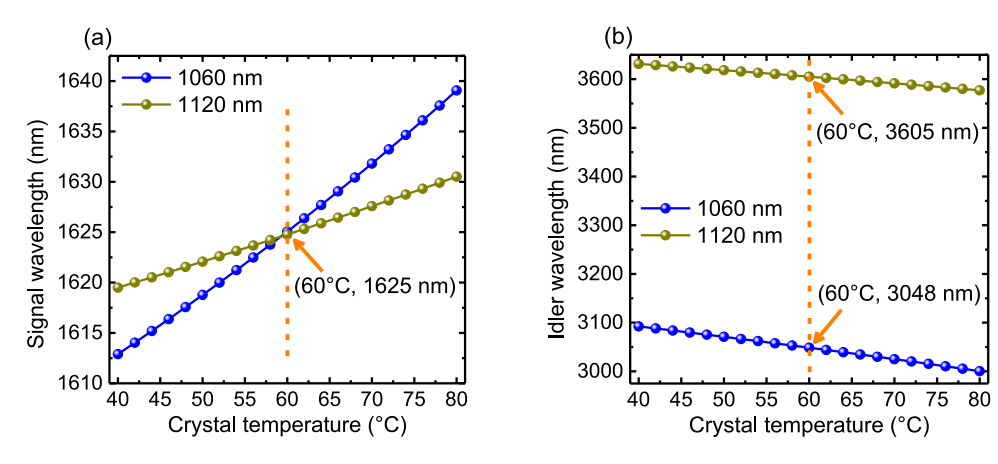


Fig. 2. Simulated tuning curves in the (a) signal and (b) idler range under 1060/1120 nm pumping conditions.

longer than the simulation results, which was caused by the thermal effect of PPLN crystal if the oven was just set at 60 °C. To achieve excellent phase-matching conditions for the intracavity DFG process, the measured signal wavelength rather than the setting value of the oven was considered as the sign of the practical crystal temperature. Thus, in order to "activate" the PPLN crystal, the OPO was gradually heated and pumped only by the 1060 nm FL. In the experiment, the pump and signal spectra were measured using the spectrometer from YOKOGAWA company with the model of AQ6370D while the idler spectrum was measured using a wavemeter from Bristol Instrument with the model of 671A. Two power meters from Thorlabs company with the model of S322C and S350C were used for confirming the pump power and parametric power (including signal and idler beams) separately. The measured signal and idler spectra under the maximum pump power as well as the output power curve were shown in Fig. 3. The central wavelength of the signal beam was 1624 nm and its full width at half maximum (FWHM) was calculated to be 80 pm. The corresponding idler wavelength was 3060 nm and its FWHM was about 13 nm as shown in Fig. 3(b). Limited by the temperature control precision of the oven, it was hard to control the signal wavelength exactly the same as the simulation results. However, the actual temperature of PPN crystal can be calculated using Sellmeier equations [11]. As shown in Fig. 3(c) which was simulated signal wavelength versus the PPLN temperature, the PPLN temperature corresponding to 1624 nm signal beam was 58 °C. Therefore, the relative conversion efficiency of intracavity DFG process can be stimulated and was shown in Fig. 3(d). The figure reveals that the peak value of the efficiency curve was just around 1120 nm, indicating that the 1624 nm signal beam was suitable for achieving highly-efficient intracavity DFG of 112 nm pump beam. Thus, it can be confirmed that the OPO system has been "activated" and in the proper status for the intracavity DFG. Fig. 3(e) was the output power curve under 1060 nm pumping and the calculated conversion efficiency. The pumping threshold was about 14 W and the maximum idler power reached 11 W, indicating a 16.5% pump-to-idler conversion efficiency. The slope efficiency was about 20.6% and the growth trend was very steady. For realizing highly-efficient DFG, the 1060 nm pump power remained the maximum in the following experiment.

After the 1060 nm pump beam built the steady oscillation, the low-power pulsed 1120 nm pump beam was incident into the resonant cavity. In the experiment, the repetition rate and pulse width of the 1120 nm FL was set as several combinations including 20 kHz & 10  $\mu$ s, 20 kHz & 6  $\mu$ s, 10 kHz & 20  $\mu$ s, 10 kHz & 10  $\mu$ s and 10 kHz & 50  $\mu$ s. The corresponding 1120 nm average pump power was measured to be 1.75 W, 0.94 W, 2.09 W, 0.81 W and 5.96 W separately. The maximum peak power was calculated to be 8.75 W, 7.83 W, 10.45 W, 8.1 W and 11.92 W. In the experiment, the pulsed 1120 nm pump wave was successfully transformed to the mid-infrared range under all temporal characteristics. The measured signal and idler spectra under different

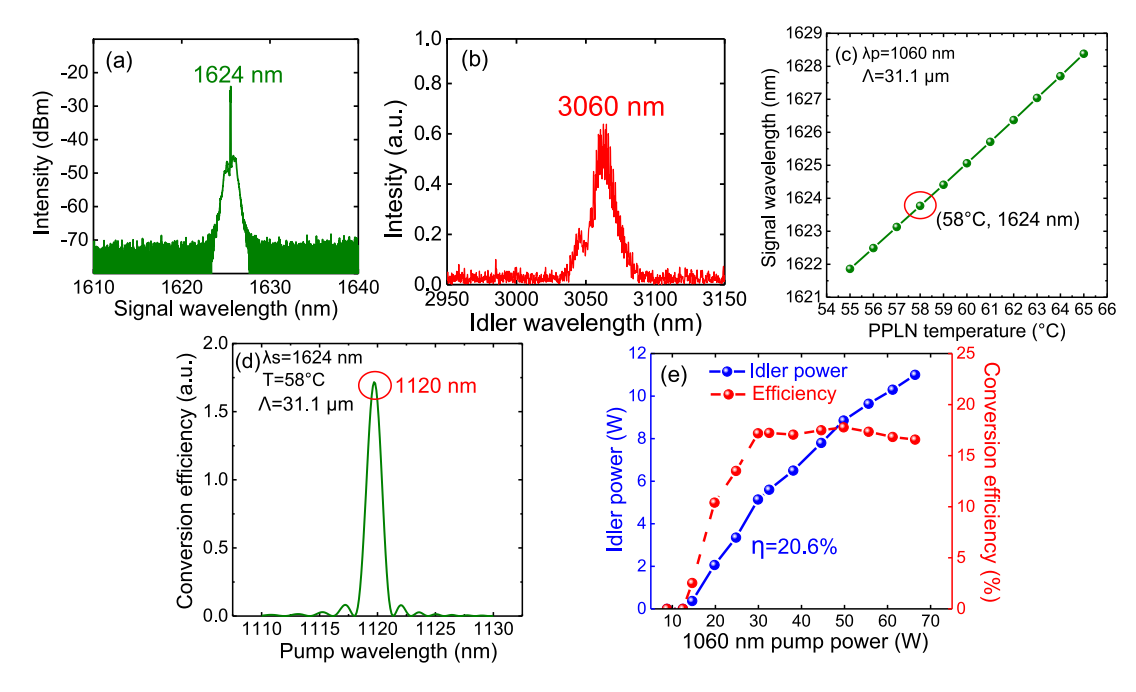


Fig. 3. Measured (a) signal spectrum, (b) idler spectrum under the maximum pump power and (e) the output power curve when the OPO was pumped only by the high-power 1060 nm FL; simulated (c) signal wavelength versus PPLN temperature and (d) relative conversion efficiency of intracavity DFG process versus the pump wavelength.

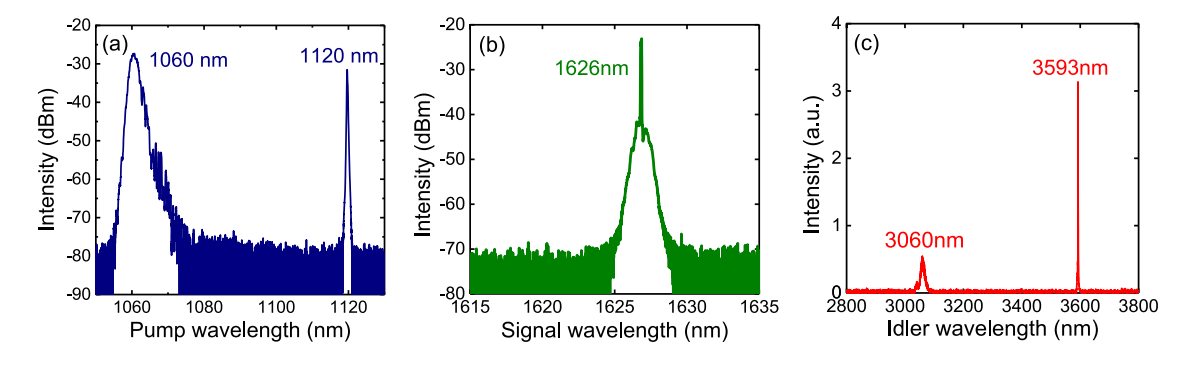


Fig. 4. Measured (a) DW pump, (b) typical signal and (c) typical DW idler spectra under different pumping conditions.

pumping conditions were almost the same. Fig. 4 reveals the DW pump spectrum and typical parametric spectra. As can be seen from Fig. 4(a) that two peaks exist in the DW pump spectra which were 1060 nm and 1120 nm. The FWHM of 1120 nm pump wave was calculated to be 0.2 nm, much narrower than that of 1060 nm pump wave which was 2.17 nm. Under all pumping conditions, just one signal beam was detected and located at 1626 nm as shown in Fig. 4(b). Like Fig. 3(a), the signal beam remained narrow-linewidth and had the FWHM of about 90 pm. It was 2 nm longer than that shown in Fig. 3(a), which was also caused by the thermal effect of the PPLN crystal. However, taking the acceptance bandwidth of DFG into consideration, the 1626 nm signal wave wouldn't severely lower the conversion efficiency. Fig. 4(c) reveals that the measured idler spectrum had two peaks locating at 3060 nm and 3593 nm. It was apparently that the newly appeared 3593 nm idler wave was generated by the pulsed 1120 nm pump wave and

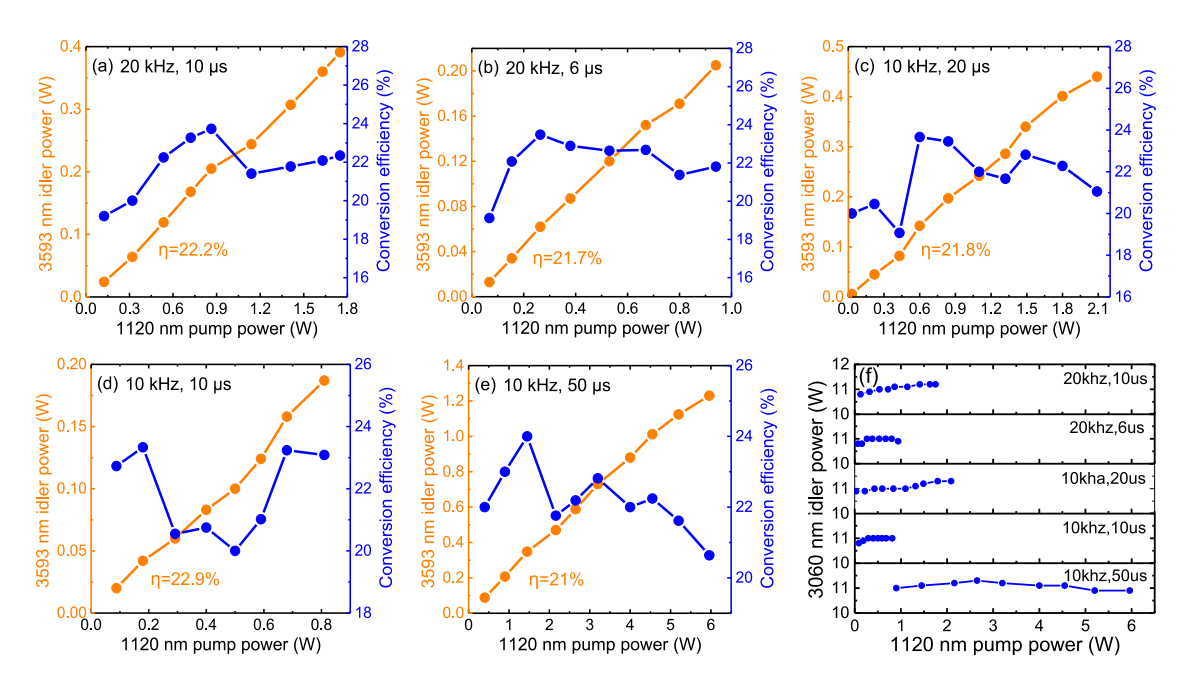


Fig. 5. (a)—(e): Measured 3593 nm idler power and calculated pump-to-idler conversion efficiency under different pumping conditions; (f) Measured 3060 nm idler power under different pumping conditions.

its bandwidth was much narrower than the 3060 nm idler wave. The conclusion can be drawn from Fig. 4(b) and (c) that both the 1060 nm and 1120 nm pump waves shared the same signal wave and realized frequency down-conversion. As can be seen that both the average power and peak power of 1120 nm pump wave didn't reach the OPO's pumping threshold. In other words, it was totally impossible for the 1120 nm pump wave to build independent parametric oscillation, which ensured that the 3593 nm idler beam was completely generated by the intracavity DFG between 1120 nm pump beam and 1626 nm signal beam. It seems like that the intensity of 3593 nm idler beam was much stronger than the 3060 nm idler beam as shown in Fig. 4(c). It didn't match with the reality and was caused by the display error of the wavemeter which was used for mid-infrared spectral detection. The wavelength location of every idler beam measured by this wavemeter was exactly correct. However, the intensity difference between different idler beams was not correct compared with the real conditions. It can be confirmed by measuring the actual power of different idler beams. In the following discussion, the 3060 nm and 3593 nm idler beams were separated using a dichroic mirror and their own power was analyzed in detail.

To research the conversion efficiency of the intracavity DFG in detail, two idler beams were separated using a dichroic mirror which was AR coated over 2.8  $\sim$  3.2  $\mu m$  and HR coated over 3.3  $\sim$  4  $\mu m$ . The 3593 nm idler power versus the 1120 nm pump power and the calculated pump-to-idler conversion efficiency was measured under different temporal characteristics and was drawn in Fig. 5(a)-(f). The figures reveal that no matter what the temporal characteristics of 1120 nm pump beam was, it was transformed to 3593 nm idler beam at every power level. The minimum down-conversion average power of 1120 nm pump beam was 125 mW, 68 mW, 30 mW, 88 mW and 400 mW separately for different temporal characteristics. The 3593 nm idler power curve showed almost linear and very steady growth trend and the slope efficiency for each situation was over 21%. It can be easily speculated that higher idler power can be obtained via increasing 1120 nm pump power. The maximum idler power under each pumping conditions was 0.39 W, 0.21 W, 0.44 W, 0.19 W and 1.23 W. The pump-to-idler conversion efficiency of each pumping condition at every power level was also calculated and drawn in Fig. 5(a)–(f). As can be seen that no matter what the temporal characteristics and pump power of 1120 nm FL was, the pump-to-idler conversion efficiency kept

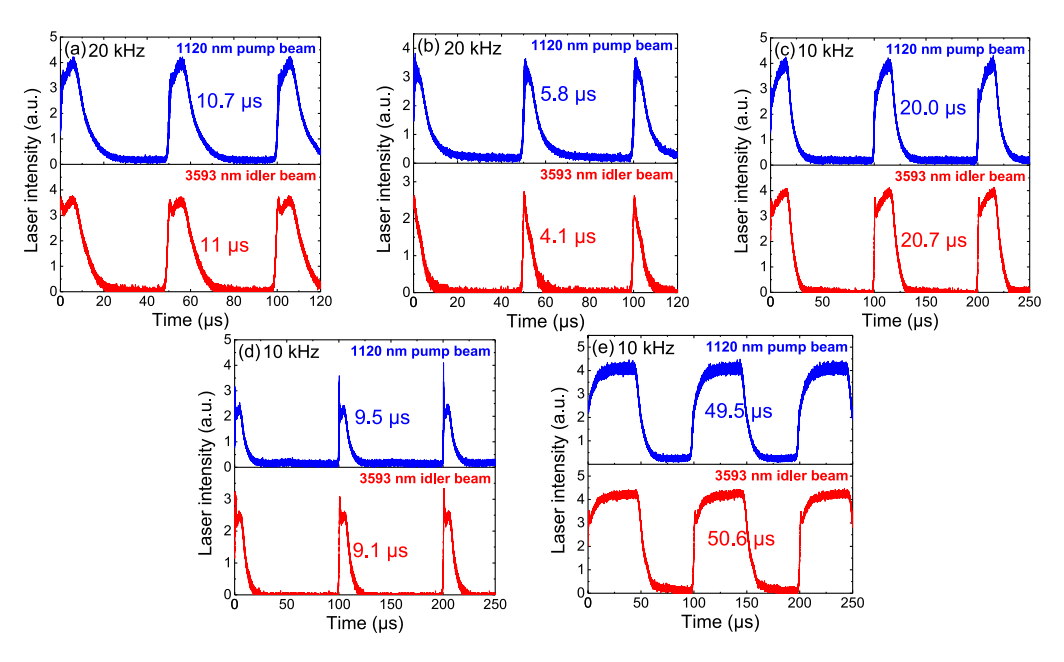


Fig. 6. Measured temporal characteristics of 1120 nm pump beam and 3593 nm idler beam.

at or above 20% except for few power points and had no significant changes. Both the conversion efficiency and minimum down-frequency power presented in the experimental results was high enough and remarkable compared with the traditional single-pass DFG setup. Some special FLs such as single-frequency FL, high-speed frequency-swept FL and ultra-short pulsed FL are of great use if they are converted to mid-infrared range. However, it is very difficult for them to realize power amplification using MOPA to pump the OPO independently or participate in single-pass DFG. This experiment offered an effective method for these low-power special FLs to realize efficient frequency down-conversion by adopting phase-matched DFG process inside high-power-CW-FL-pumped OPOs. Fig. 5(f) was the measured 3060 nm idler power under different 1120 nm pump power and temporal characteristics. As can be seen from the figure that the 3060 nm idler power always kept around 11 W and had very small fluctuation in the whole experiment when the intracavity DFG occurred. The stable 3060 nm idler power symbolized the stable intracavity signal power and greatly guaranteed the stability of conversion efficiency of the intracavity DFG.

The temporal characteristics of 1120 nm pump beam and 3593 nm idler beam under different pumping conditions were also measured. The detector used for measuring the 1120 nm pump beam was a fiber-coupled InGaAs biased photoelectric detector from Thorlabs company with the model of DET08CFC. Its wavelength and bandwidth was 800  $\sim$  1700 nm and 5 GHz. The detector used for measuring the 3593 nm idler beam was a InAsSb-based amplified photoelectric detector from Thorlabs company and its model was PDA07P2. Its wavelength and bandwidth was  $2.7 \sim 5.3 \ \mu m$  and 9 MHz. The corresponding oscilloscope was from Tektronix company with the model of MDO3000. The measured results were drawn in Fig. 6. The time value marked on the figures represented calculated pulse width of the corresponding beams. Except for Fig. 6(b), the pulse width of pump and idler beams was almost the same and the minute difference between them was considered as the measurement and calculation error. In Fig. 6(b), the pulse width of 3593 nm idler beam was much narrower than the 1120 nm pump beam. It was analyzed that the 1120 nm peak power under this situation was the lowest among all five situations. Part of the 1120 nm pump beam was unable to overcome the transmission loss and achieve frequency down-conversion with the intracavity signal beam, and thus resulted in shorter pulse width. However, it's just our preliminary qualitative analysis and maybe was not matched well with the truth. More detailed

theoretical analysis will be conducted in the further research. Except for the difference in pulse width, the pulse shape of 3593 nm idler beam was also very similar to the 1120 nm pump beam and revealed excellent stability in maintaining pulse shape of pump beam. This result was very promising in long-distance communication using waveform-modulated mid-infrared laser which can be converted from pulsed laser around 1  $\mu$ m via the highly-efficient intracavity DFG shown in this paper.

## 4. Conclusion

In conclusion, for the first time, we demonstrated highly-efficient pulsed mid-infrared generation based on the intracavity DFG in a CW-FL-pumped mid-infrared OPO. Different from the direct frequency mixing, the intracavity difference frequency mixing adopted a high-power 1  $\mu$ m fiber laser, rather than the 1.5  $\mu$ m fiber laser, to pump an OPO and CW high-power, high-brightness signal beam around 1.5  $\mu$ m was obtained inside the resonant cavity which was coaxial with 1  $\mu$ m laser. Therefore, the aimed low-power 1 µm laser source can be incident into the resonant cavity together with the high-power 1  $\mu$ m fiber laser using a WDM and then interact with the intracavity 1.5  $\mu$ m signal beam. The originality of this method has been proved effective in our previous reports and worked excellently as well in this experiment. The low-power pulsed near-infrared FL was located at 1120 nm and a high-power CW 1060 nm FL was adopted as the assistant laser for building parametric oscillation and producing intracavity signal beam. The pulse width and repetition rate of 1120 nm FL was set at five different combinations to research the intracavity DFG under different pumping conditions. Similar to our previous reports, the signal wavelength was adjusted to a specific value by controlling the PPLN temperature for ensuring that both the OPO and DFG processes satisfy phase-matching conditions. By interacting with high-power intracavity signal beam, the 1120 nm pump beam was successfully transformed to 3593 nm idler beam at every pumping condition even when the 1120 nm average power was just tens of milliwatts. Both the pump-to-idler conversion efficiency and slope efficiency was over 20% under every pumping conditions, which was high enough compared with the traditional single-pass DFG schemes. What can foreknow is that better results can be obtained by optimizing the phase mismatch of intracavity DFG process. The temporal characteristics of 1120 nm pump beam and 3593 nm idler beam were also studied in detail. Except for one pumping situation, the pulse width of pump and idler beams was basically equal under every pumping conditions. In addition, the pulse shape of idler beams was very similar to the pump beams under every pumping conditions. All the experiment results displayed tremendous potential in frequency down-conversion of low-power FLs with particular characteristics and long-distance communication using waveform-modulated mid-infrared laser. Next research will be focused on increasing conversion efficiency of intracavity DFG process and the effectiveness of this method in frequency conversion of other kinds of special FLs.

# References

- [1] S. D. Jackson, "Towards high-power mid-infrared emission from a fibre laser," Nature Photon., vol. 6, pp. 423, Jul. 2012.
- [2] C. Frerichs and U. B. Unrau, "Passive Q-Switching and mode-locking of erbium-doped fluoride fiber lasers at 2.7 μm," Opt. Fiber Technol., vol. 2, pp. 358–366, Oct. 1996.
- [3] V. Fortin et al., "Towards the development of fiber lasers for the 2 to 4 μm spectral region," Opt. Eng., vol. 52, May 2013, Art. no. 054202.
- [4] J. G. Crowder, H. R. Hardaway, and C. T. Elliott, "Mid-infrared gas detection using optically immersed, room-temperature, semiconductor devices [J]," *Meas. Sci. Technol.*, vol. 13, no. 6, 2002, Art. no. 882.
- [5] Y. Peng et al., "High-power, narrow-bandwidth mid-infrared PPMgLN optical parametric oscillator with a volume Bragg grating," Opt. Exp., vol. 23, no. 24, pp. 30827–30832, 2015.
- [6] Š. Parsa, S. C. Kumar, K. Devi, and M. Ebrahim-Zadeh, "High-power, high-beam-quality, idler-resonant mid-infrared picosecond optical parametric oscillator," in *High-Brightness Sources and Light-driven Interactions*, OSA Technical Digest (online) (Optical Society of America, 2018), Paper MW2C.6.
- [7] P. Belden, D. W. Chen, and F. D. Teodoro, "Watt-level, gigahertz-linewidth difference-frequency generation in PPLN pumped by an nanosecond-pulse fiber laser source," *Opt. Lett.*, vol. 40, no. 6, pp. 958–961, 2015.
- [8] R. T. Murray, T. H. Runcorn, E. J. R. Kelleher, and J. R. Taylor, "Highly efficient mid-infrared difference-frequency generation using synchronously pulsed fiber lasers," *Opt. Lett.*, vol. 41, no. 11, pp. 2446–2449, 2016.

- [9] C. Xi et al., "Highly efficient continuous-wave mid-infrared generation based on intracavity difference mixing," High
- Power Laser Sci. Éng., vol. 7, no. e67, pp. 1–5, 2019.

  [10] Y. Shang, J. Xu, P. Wang, X. Li, P. Zhou, and X. Xu, "Ultra-stable high-power mid-infrared optical parametric oscillator pumped by a super-fluorescent fiber source," *Opt. Exp.*, vol. 24, no. 19, pp. 21684–21692, 2016.

  [11] O. Paul *et al.*, "Temperature-dependent sellmeier equation in the MIR for the extraordinary refractive index of 5% MgO
- doped congruent linbO<sub>3</sub>," Appl. Phys. B, vol. 86, no. 1, pp. 111–115, 2007.